

OPTIMUM DESIGN OF DAMPED VIBRATION ABSORBER FOR ROTATIONALLY PERIODIC STRUCTURES

A. A. Ghaderi A. Mohammadzadeh* M. N. Bahrami

*Department of Mechanical and Aerospace Engineering
Science and Research Branch
Islamic Azad University
Tehran, Iran*

ABSTRACT

In this study, a damped centrifugally driven order-tuned vibration absorber designed for vibration reduction in rotating flexible structures, bladed disk assemblies and blisk such as turbine blades, compressor and fan blades, pump and helicopter rotor blades *etc.* during steady operation with constant speed and under engine order excitation (e.o excitation). Effect of mistuning is disregarded. System is assumed with fully cyclic symmetry. The disk is imposed as being rigid. Elastic behavior for blades is supposed. A model with two degree of freedom is extracted for the blades. Each blade is fitted with nominally identical damped order-tuned vibration absorber that is moved in a circular path. Aerodynamic damping and coupling effects between the blades are considered. Optimal values of parameters of the absorber, to suppress blade vibration especially in resonance condition, are derived by Genetic Algorithm (GA) and MATLAB software. H_2 optimization criterion is used. It is observed that with the deviation of each parameter from the optimal condition, the system response is moved away from the ideal design situation and all of the absorbers' design parameters have definite effects on the system frequency response and on the dissipated energy during vibration. Therefore, ignorance of the effect of one of those parameters (which was happened in literature) affected the system response completely. Literature is reviewed and validity of the results is confirmed.

Keywords: Order tuned vibration absorber, Damping, Rotationally periodic structure, Optimization.

1. INTRODUCTION

In recent years and due to financial and irrecoverable life damages, prevention of failure in rotating machines is vitally important. Many researches, by introducing the phenomenon of high cycle fatigue as the main cause of failure, have been determined blade as a critical component of machines [1-6]. Among researches performed by studying blade vibration under different condition [7-10], which have been provided diverse methods to reduce blade vibrations [11-14], centrifugal pendulum vibration absorber is a proper way to suppress blade vibration especially in resonance condition [15,16].

These absorbers exploit the centrifugal field arising from rotation so that they are tuned to a given order of rotation, rather than to a fixed frequency. By tuning each undamped absorber within a small but finite range, known as no resonance zone, resonance can be avoid for systems with cyclic symmetry [17,18]. In this investigation, the importance of damping is considered and effect of damping of centrifugally driven order-tuned vibration absorber on blade vibration is studied.

The effects of mistuning are neglected then the system is considered with fully cyclic symmetry and the disk is assumed as being rigid. The blade is assumed elastic and with the use of lumped parameter method, a model with two degree of freedom is extracted for the blades. Each of the blades, is equipped with a damped order-tuned vibration absorber that is moved in a circular path. The optimal values of the length of the pendulum, mass and damping of the absorber in the presence of coupling between the blades and aerodynamic damping are determined by the using of GA and MATLAB software. In order to determine optimal values of parameters the H_2 optimization criterion is used. The objective is to reduce the total vibration energy of the system over all frequency. In this optimization criterion, the area (called H_2 norm) under frequency response curve of the system is minimized [19].

2. FORMULATION

The system is assumed as being perfectly tuned, and consequently, is modelled as an identical, identically

* Corresponding author (a-mohammadzadeh@srbiau.ac.ir)

coupled of N blades, which are uniformly attached to a rigid disk. The effects of temperature increases and the occurrence of creep phenomenon are omitted and the system behavior is assumed linear. Gyroscopic and eccentricity forces are neglected and intact blades with constant material property and thickness are modelled as elastic Euler-Bernoulli cantilever beams. Transverse vibration of beams is studied and a model with two degree of freedom is extracted. As a result, according to Fig. 1 the provided model is included N double pendulums with the lengths of L_a and L_b and the lumped masses of M_a and M_b . These pendulums are uniformly pinned to the surroundings of a rigid disk with a radius of H , which are rotated with the constant speed of Ω around the axis through A .

The flexural stiffness of each blades are modeled with a linear torsional springs in points a and b and inter-blade coupling and aerodynamic damping is modeled in the distances of r_a and r_b and with linear springs and dampers [18]. The blade's dynamics are shown with the coordinates of θ_a and θ_b . When blades are in a fully radial configuration, or when for each blade, $\theta_a = \theta_b = 0$ the dampers and springs are unstressed. Identical absorbers which includes a pendulum with a lumped mass of m and a length of d_b are fitted in the each of the blades and the effects of the damping of absorber is modelled using a torsional damper acts at attachment point of absorber pendulum to the blade (Point P). The coordinate of β_b is described the dynamic of an absorber to its corresponding blade. Figure 2 shows the blade and the absorber fitted in it along with the corresponding part on the disk constituted a sector.

Table 1 introduces the terms related to blade and absorber.

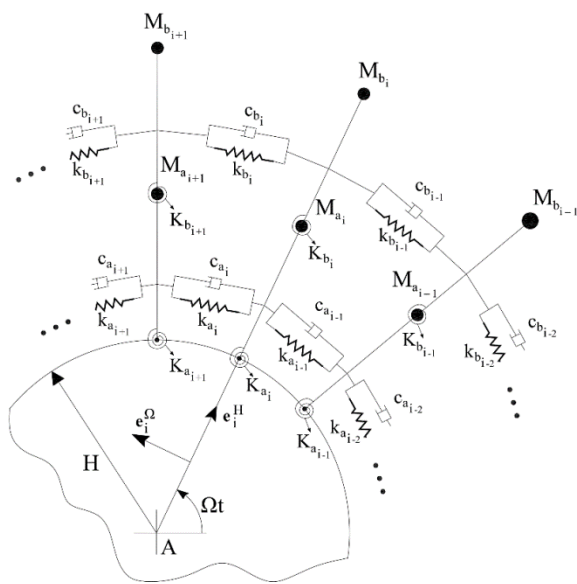


Fig. 1 Lumped parameter model of flexible rotating blades (in [18] they have assigned 1 Dof to the disk and another one to the blade).

In order to study the system frequency response, the kinetic energy of the entire system (N blades to each an absorber is fitted) is extracted according to Eq. (1)

$$T = \sum \frac{1}{2} M_{a_i} \left(H^2 \Omega^2 + L_{a_i}^2 (\Omega + \dot{\theta}_{a_i})^2 + 2H\Omega L_{a_i} (\Omega + \dot{\theta}_{a_i}) \cos(\theta_{a_i}) \right) + \frac{1}{2} M_{b_i} \left(H^2 \Omega^2 + L_{a_i}^2 (\Omega + \dot{\theta}_{a_i})^2 + L_{a_i}^2 (\Omega + \dot{\theta}_{a_i} + \dot{\theta}_{b_i})^2 + 2H\Omega L_{a_i} (\Omega + \dot{\theta}_{a_i}) \cos(\theta_{a_i}) + 2H\Omega L_{b_i} (\Omega + \dot{\theta}_{a_i} + \dot{\theta}_{b_i}) \cos(\theta_{a_i} + \theta_{b_i}) + 2L_{a_i} L_{b_i} (\Omega + \dot{\theta}_{a_i}) (\Omega + \dot{\theta}_{b_i}) \cos(\theta_{b_i}) \right) + \frac{1}{2} m_{b_i} \left(H^2 \Omega^2 + L_{a_i}^2 (\Omega + \dot{\theta}_{a_i})^2 + \alpha_{b_i}^2 L_{b_i}^2 (\Omega + \dot{\theta}_{a_i} + \dot{\theta}_{b_i})^2 + d_{b_i}^2 (\Omega + \dot{\theta}_{a_i} + \dot{\theta}_{b_i} + \dot{\beta}_{b_i})^2 + 2H\Omega L_{a_i} (\Omega + \dot{\theta}_{a_i}) \cos(\theta_{a_i}) + 2\alpha_{b_i} L_{b_i} H\Omega (\Omega + \dot{\theta}_{a_i} + \dot{\theta}_{b_i}) \cos(\theta_{a_i} + \theta_{b_i}) + 2H\Omega d_{b_i} (\Omega + \dot{\theta}_{a_i} + \dot{\theta}_{b_i} + \dot{\beta}_{b_i}) \cos(\theta_{a_i} + \theta_{b_i} + \beta_{b_i}) + 2\alpha_{b_i} L_{a_i} L_{b_i} (\Omega + \dot{\theta}_{a_i}) (\Omega + \dot{\theta}_{a_i} + \dot{\theta}_{b_i}) \cos(\theta_{b_i}) + 2L_{a_i} d_{b_i} (\Omega + \dot{\theta}_{a_i}) (\Omega + \dot{\theta}_{a_i} + \dot{\theta}_{b_i} + \dot{\beta}_{b_i}) \cos(\theta_{b_i} + \beta_{b_i}) + 2\alpha_{b_i} L_{a_i} d_{b_i} (\Omega + \dot{\theta}_{a_i} + \dot{\theta}_{b_i}) (\Omega + \dot{\theta}_{a_i} + \dot{\theta}_{b_i} + \dot{\beta}_{b_i}) \cos(\beta_{b_i}) \right) \quad (1)$$

Gravitational effect is ignored so the system potential energy due to the flexural stiffness of the blades and elastic inter-blade coupling are given by Eq. (2)

$$V = \sum_{i=1}^N \frac{1}{2} K_{a_i} \theta_{a_i}^2 + \frac{1}{2} k_{a_i} r_{a_i}^2 (\theta_{a_{i+1}} - \theta_{a_i})^2 + \frac{1}{2} k_{a_{i-1}} r_{a_i}^2 (\theta_{a_i} - \theta_{a_{i-1}})^2 + \frac{1}{2} K_{b_i} \theta_{b_i}^2 + \frac{1}{2} k_{b_i} \left((L_{a_i} + r_{b_i}) \theta_{a_{i+1}} + r_{b_i} \theta_{b_{i+1}} - L_{a_i} \theta_{a_i} - r_{b_i} \theta_{b_i} \right)^2 + \frac{1}{2} k_{b_{i-1}} \left((L_{a_i} + r_{b_i}) \theta_{a_i} + r_{b_i} \theta_{b_i} - (L_{a_i} + r_{b_i}) \theta_{a_{i-1}} - r_{b_i} \theta_{b_{i-1}} \right)^2 \quad (2)$$

Finally, according to Eq. (3), the Rayleigh dissipation function describes the damping of the absorber and the aerodynamic damping

$$R = \sum_{i=1}^N \frac{1}{2} c_{a_i} r_{a_i}^2 (\dot{\theta}_{a_{i+1}} - \dot{\theta}_{a_i})^2 + \frac{1}{2} c_{a_{i-1}} r_{a_i}^2 (\dot{\theta}_{a_i} - \dot{\theta}_{a_{i-1}})^2 + \frac{1}{2} c_{b_i} \left((L_{a_i} + r_{b_i}) \dot{\theta}_{a_{i+1}} + r_{b_i} \dot{\theta}_{b_{i+1}} - L_{a_i} \dot{\theta}_{a_i} - r_{b_i} \dot{\theta}_{b_i} \right)^2 + \frac{1}{2} c_{b_{i-1}} \left((L_{a_i} + r_{b_i}) \dot{\theta}_{a_i} + r_{b_i} \dot{\theta}_{b_i} - (L_{a_i} + r_{b_i}) \dot{\theta}_{a_{i-1}} - r_{b_i} \dot{\theta}_{b_{i-1}} \right)^2 + \frac{1}{2} C_{\beta_i} \dot{\beta}_{a_i}^2 \quad (3)$$

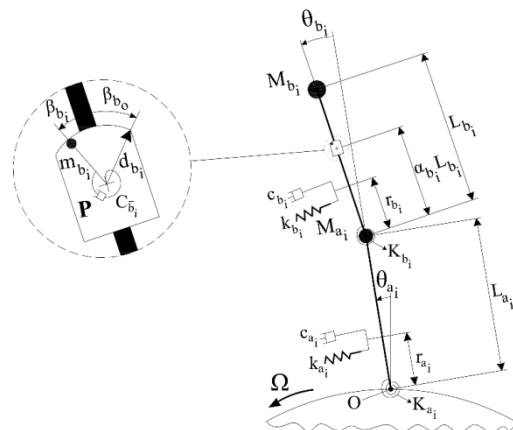


Fig. 2 Sector model of flexible rotating blades (in [18] they have assigned 1 DOF to the disk and another one to the blade).

Table 1 List of variables and parameters of blade and absorber.

| Parameter | Description | Unit |
|------------|---|-------|
| Ω | Angular speed | Rad/s |
| θ_a | Blade angle | Rad |
| θ_b | Blade angle | Rad |
| β_b | Absorber angle | Rad |
| H | Radius of the disk | m |
| L_a | Length of the blade | m |
| L_b | Length of the blade | m |
| L | Blade total length | m |
| d_b | Length of the absorber | m |
| r_a | Distance from base of blade to coupling spring and aerodynamic damping attachment point | m |
| r_b | Distance from middle of blade to coupling spring and aerodynamic damping attachment point | m |
| M | Blade total mass | Kg |
| M_a | Blade lumped mass | Kg |
| M_b | Blade lumped mass | Kg |
| m | Absorber mass | Kg |
| K | Blade stiffness | N/m |
| K_a | Blade lumped stiffness | N/m |
| K_b | Blade lumped stiffness | N/m |
| k_a | Stiffness coupling between sectors | N/m |
| k_b | Stiffness coupling between sectors | N/m |
| c_a | Damping coupling between sectors | N.s/m |
| c_b | Damping coupling between sectors | N.s/m |
| C_b | Absorber damping | N.s/m |

The blades are harmonically forced in the transverse sense, such that the cyclic system is circumferentially forced by a TW, by e.o excitation of order n . To focus on the optimization problem, the range of $0 < n < N$ is considered for the excitation order. The values of $n \geq N$, will not affect the solution method quality and the results. The e.o excitation is modeled with the Eq. (4)

$$\begin{aligned}
 Q_i^{(\theta_a)} &= F_o L_{a_i} e^{j\theta_i} e^{jn\Omega t} \\
 Q_i^{(\theta_b)} &= F_o L_{b_i} e^{j\theta_i} e^{jn\Omega t} \\
 Q_i^{(\beta_b)} &= 0
 \end{aligned} \tag{4}$$

In the above equations, F_o is strength of excitation and n is excitation order, Ω is rotational speed and $\theta_i = 2\pi \frac{n}{N} (i - 1)$ is inter-blade phase angle [17]. Lagrange's method is employed and the equations of motion are extracted. To extract the dimension-less form of the equations, the time is rescaled according to $\tau = \omega_o t$ and $\omega_o = \sqrt{\frac{K}{ML^2}}$ is the undamped natural frequency of 1Dof model of single isolated blade. Finally, the parameters that are defined in Table 2 are considered

Table 2 Descriptions and values of dimensionless variables and parameters

| Parameter | Description | Value |
|---|--|--------------|
| $\sigma = \Omega/\omega_o$ | Angular speed of the rotor | [0-1] |
| $\mu_a = M_a/M$ | Lumped mass of the blade | 0.25 |
| $\mu_b = M_b/M$ | Lumped mass of the blade | 0.00014 |
| $\mu_{\bar{b}} = m_b/M$ | Mass of the absorber | [0.001-0.01] |
| $\rho_a = L_a/L$ | Blade pendulum length | 0.5 |
| $\rho_b = L_b/L$ | Blade pendulum length | 0.5 |
| $\rho_{\bar{b}} = d_b/L$ | Absorber pendulum length | [0.01-0.15] |
| $\delta = H/L$ | Radius of the disk | 0.67 |
| $f_a = F_o L_a/K$ | Strength of e.o excitation | 0.016 |
| $f_b = F_o (L_a + L_b)/K$ | Strength of e.o excitation | 0.001 |
| $\xi_{\bar{a}} = (c_a r_a^2 + c_b (L_a + r_b)^2) / (L^2 \sqrt{MK/L^2})$ | Aerodynamic damping constant | 0.0005 |
| $\xi_{\bar{b}} = (c_b (L_a + r_b) r_b) / (L^2 \sqrt{MK/L^2})$ | Aerodynamic damping constant | 0.0001 |
| $\xi_c = (c_b r_b^2) / (L^2 \sqrt{MK/L^2})$ | Aerodynamic damping constant | 0.0001 |
| $\xi_{\bar{b}} = (C_b) / (L^2 \sqrt{MK/L^2})$ | Absorber damping constant | [0-1000] |
| $v_a = \sqrt{K_a/K}$ | Blade torsional stiffness | 0.1 |
| $v_b = \sqrt{K_b/K}$ | Blade torsional stiffness | 0.5 |
| $v_c = \sqrt{(k_a r_a^2 + k_b (L_a + r_b)^2) / K}$ | Strength of the coupling between blades | 0.5 |
| $v_d = \sqrt{(k_b (L_a + r_b) r_b) / K}$ | Strength of the coupling between blades | 0.1 |
| $v_e = \sqrt{k_b r_b^2 / K}$ | Strength of the coupling between blades | 0.1 |
| α_b | Distance from middle of blade (point b) to the absorber base point P | 0.8 |

and dimension-less form of the equations are linearized for small blades and absorbers motions and extracted as Eqs. (5) to (7).

For 1st Dof

$$\begin{aligned}
 &\mu_a (\rho_a^2 \theta_{a_i}'' + \delta \rho_a \sigma^2 \theta_{a_i}) + \mu_b (\rho_b^2 \theta_{b_i}'' + \rho_{\bar{b}}^2 (\theta_{a_i}'' + \theta_{b_i}'') + \\
 &2\rho_a \rho_b \theta_{a_i}'' + \rho_a \rho_b \theta_{b_i}'' + \delta \rho_a \sigma^2 \theta_{a_i} + \delta \rho_b \sigma^2 (\theta_{a_i} + \theta_{b_i})) + \\
 &\mu_{\bar{b}} (\rho_{\bar{b}}^2 \theta_{a_i}'' + \alpha_{\bar{b}}^2 \rho_{\bar{b}}^2 (\theta_{a_i}'' + \theta_{b_i}'') + \rho_{\bar{b}}^2 (\theta_{a_i}'' + \theta_{b_i}'' + \beta_{b_i}'') + \\
 &2\alpha_b \rho_b \rho_a \theta_{a_i}'' + \alpha_b \rho_b \rho_a \theta_{b_i}'' + 2\rho_{\bar{b}} \rho_a \theta_{a_i}'' + \rho_{\bar{b}} \rho_a (\theta_{a_i}'' + \beta_{b_i}'') + \\
 &2\alpha_b \rho_{\bar{b}} \rho_b (\theta_{a_i}'' + \beta_{b_i}'') + \alpha_b \rho_{\bar{b}} \rho_b (\beta_{b_i}'') + \delta \rho_b \sigma^2 (\theta_{a_i} + \\
 &\delta \alpha_b \rho_b \sigma^2 (\theta_{a_i} + \theta_{b_i}) + \delta \rho_{\bar{b}} \sigma^2 (\theta_{a_i} + \theta_{b_i} + \beta_{b_i})) + v_a^2 (\theta_{a_i}) + \\
 &\xi_a (\theta_{a_i}') + (\xi_{\bar{a}} (-\theta_{a_{i-1}} + 2\theta_{a_i} - \theta_{a_{i+1}}) + \xi_{\bar{b}} (-\theta_{b_{i-1}} + 2\theta_{b_i} - \\
 &\theta_{b_{i+1}})) + (v_c^2 (-\theta_{a_{i-1}} + 2\theta_{a_i} - \theta_{a_{i+1}}) + v_d^2 (-\theta_{b_{i-1}} + 2\theta_{b_i} - \\
 &\theta_{b_{i+1}})) = f_a e^{j\phi_i} e^{jn\sigma\tau}
 \end{aligned} \tag{5}$$

For 2nd Dof

$$\begin{aligned} & \mu_b \left(\rho_a \rho_b \theta_{a_i}'' + \rho_b^2 (\theta_{a_i}'' + \theta_{b_i}'') + \delta \rho_b \sigma^2 (\theta_{a_i} + \theta_{b_i}) + \rho_a \rho_b \sigma^2 (\theta_{b_i}) \right) + \mu_b \left(\alpha_b^2 \rho_b^2 (\theta_{a_i}'' + \theta_{b_i}'') + \rho_b^2 (\theta_{a_i}'' + \theta_{b_i}'' + \beta_{b_i}'') + \right. \\ & \alpha_b \rho_b \rho_a (\theta_{a_i}'') + \rho_b \rho_a (\theta_{a_i}'' + \beta_{b_i}'') + 2\alpha_b \rho_b \rho_b (\theta_{a_i}'' + \beta_{b_i}'') + \alpha_b \rho_b \rho_b (\beta_{b_i}'') + \delta \alpha_b \rho_b \sigma^2 (\theta_{a_i} + \theta_{b_i}) + \delta \rho_b \sigma^2 (\theta_{a_i} + \theta_{b_i} + \beta_{b_i}) \\ & \left. + \alpha_b \rho_a \rho_b \sigma^2 \theta_{b_i} + \rho_a \rho_b \sigma^2 (\theta_{b_i} + \beta_{b_i}) \right) + v_d^2 (\theta_{b_i}) + \xi_b (\theta_{b_i}') + \left(\xi_b (-\theta_{a_{i-1}}' + 2\theta_{a_i}' - \theta_{a_{i+1}}') + \xi_c (-\theta_{b_{i-1}}' + 2\theta_{b_i}' - \theta_{b_{i+1}}') \right) \\ & \left. + \left(v_d^2 (-\theta_{a_{i-1}} + 2\theta_{a_i} - \theta_{a_{i+1}}) + v_e^2 (-\theta_{b_{i-1}} + 2\theta_{b_i} - \theta_{b_{i+1}}) \right) = f_b e^{j\phi_i} e^{jn\sigma\tau} \end{aligned} \quad (6)$$

And for the absorber

$$\begin{aligned} & \mu_b \left(\rho_b^2 (\theta_{a_i}'' + \theta_{b_i}'' + \beta_{b_i}'') + \rho_b \rho_a (\theta_{a_i}'') + \alpha_b \rho_b \rho_b (\theta_{a_i}'' + \theta_{b_i}'') + \delta \rho_b \sigma^2 (\theta_{a_i} + \theta_{b_i} + \beta_{b_i}) + \rho_a \rho_b \sigma^2 (\theta_{b_i} + \beta_{b_i}) + \right. \\ & \left. \alpha_b \rho_b \rho_b \sigma^2 (\beta_{b_i}) + \xi_b (\beta_{a_i}') \right) = 0 \end{aligned} \quad (7)$$

Each $\mathbf{z}_i = (\theta_{a_i}, \theta_{b_i}, \beta_{b_i})^T$ as blade dynamic vector is stacked into the configuration vector $\mathbf{q} = (\mathbf{z}_1, \mathbf{z}_2, \dots, \mathbf{z}_N)^T$ so the governing matrix equation of motions for overall system is

$$\widehat{\mathbf{M}}\mathbf{q}'' + \widehat{\mathbf{C}}\mathbf{q}' + \widehat{\mathbf{K}}\mathbf{q} = \widehat{\mathbf{f}}e^{jn\sigma\tau} \quad (8)$$

where, $\widehat{\mathbf{M}}$ (overall system mass matrix), is a block diagonal matrix with blocks of \mathbf{M} (each sector mass matrix).

$$\mathbf{M} = \begin{bmatrix} \mu_a \rho_a^2 + \mu_b (\rho_a + \rho_b)^2 + \mu_b ((\rho_a + \rho_b)^2 + \alpha_b \rho_b (\alpha_b \rho_b + 2\rho_b + 2\rho_b)) & \mu_b (\rho_b (\rho_a + \rho_b)) + \mu_b ((\alpha_b \rho_b + \rho_b) (\alpha_b \rho_b + \rho_a + \rho_b)) & \mu_b ((\rho_b) (\alpha_b \rho_b + \rho_a + \rho_b)) \\ \mu_b (\rho_b (\rho_a + \rho_b)) + \mu_b ((\alpha_b \rho_b + \rho_b) (\alpha_b \rho_b + \rho_a + \rho_b)) & \mu_b \rho_b^2 + \mu_b (\alpha_b \rho_b + \rho_b)^2 & \mu_b \rho_b (\alpha_b \rho_b + \rho_b) \\ \mu_b ((\rho_b) (\alpha_b \rho_b + \rho_a + \rho_b)) & \mu_b \rho_b (\alpha_b \rho_b + \rho_b) & \mu_b \rho_b^2 \end{bmatrix} \quad (9)$$

$\widehat{\mathbf{K}} \in \mathcal{B}\mathcal{L}\mathcal{B}\mathcal{P}_{3,N}$ is the overall system stiffness matrix, which is generated with $\mathbf{K} + 2\mathbf{K}_c, -\mathbf{K}_c, \mathbf{0}, \dots, \mathbf{0}, -\mathbf{K}_c$.

\mathbf{K} is the sector stiffness matrix, which is

$$\mathbf{K} = \begin{bmatrix} \delta \sigma^2 (\mu_a \rho_a + \mu_b \rho_a (\rho_a + \rho_a) + \mu_b (\alpha_b \rho_b + \rho_a + \rho_b)) + v_d^2 & \delta \sigma^2 (\mu_b \rho_b + \mu_b (\alpha_b \rho_b + \rho_b)) & \delta \mu_b \rho_b \sigma^2 \\ \delta \sigma^2 (\mu_b \rho_b + \mu_b (\alpha_b \rho_b + \rho_b)) & (\delta + \rho_a) (\mu_b \rho_b + \mu_b (\alpha_b \rho_b + \rho_b)) \sigma^2 + v_b^2 & \mu_b \rho_b \sigma^2 (\rho_a + \delta) \\ \delta \mu_b \rho_b \sigma^2 & \mu_b \rho_b \sigma^2 (\rho_a + \delta) & \mu_b \rho_b \sigma^2 (\alpha_b \rho_b + \rho_a + \delta) \end{bmatrix} \quad (10)$$

The coupling between the blades is shown as \mathbf{K}_c matrix.

$$\mathbf{K}_c = \begin{bmatrix} v_c^2 & v_d^2 & 0 \\ v_d^2 & v_e^2 & 0 \\ 0 & 0 & 0 \end{bmatrix} \quad (11)$$

$\widehat{\mathbf{C}} \in \mathcal{B}\mathcal{L}\mathcal{B}\mathcal{P}_{3,N}$, is the overall system damping matrix and its generated elements are $\mathbf{C} + 2\mathbf{C}_c, -\mathbf{C}_c, \mathbf{0}, \dots, \mathbf{0}, -\mathbf{C}_c$. \mathbf{C} is the sector- damping matrix

$$\mathbf{C} = \begin{bmatrix} 0 & 0 & 0 \\ 0 & 0 & 0 \\ 0 & 0 & \xi_b \end{bmatrix} \quad (12)$$

And finally, the aerodynamic damping matrix, is defined as

$$\mathbf{C}_c = \begin{bmatrix} \xi_a & \xi_b & 0 \\ \xi_b & \xi_c & 0 \\ 0 & 0 & 0 \end{bmatrix} \quad (13)$$

The \mathbf{f} vector shows the force applied to each sector.

$$\mathbf{f} = \begin{bmatrix} f_a \\ f_b \\ 0 \end{bmatrix} \quad (14)$$

In terms of Circulant operators, the overall system mass, stiffness, damping and force matrices are shown as below.

$$\begin{aligned} \widehat{\mathbf{M}} &= \text{circ}(\mathbf{M}, \mathbf{0}, \mathbf{0}, \dots, \mathbf{0}, \mathbf{0}) = \text{diag}_{i \in N}(\mathbf{M}) \\ \widehat{\mathbf{C}} &= \text{circ}(\mathbf{C} + 2\mathbf{C}_c, -\mathbf{C}_c, \mathbf{0}, \dots, \mathbf{0}, -\mathbf{C}_c) \\ \widehat{\mathbf{K}} &= \text{circ}(\mathbf{K} + 2\mathbf{K}_c, -\mathbf{K}_c, \mathbf{0}, \dots, \mathbf{0}, -\mathbf{K}_c) \\ \widehat{\mathbf{f}} &= \text{circ}(\mathbf{f}e^{j\theta_1}, \mathbf{f}e^{j\theta_1}, \dots, \mathbf{f}e^{j\theta_1})^T \end{aligned} \quad (15)$$

Determining the forced response of the overall system with using of standard techniques like calculating the system impedance matrix does not offer any insight into the optimization of the absorber. Therefore, because of the cyclic symmetry of system and due to the Circulant structure of its matrices, with the use of modal transformation, the Eq. (8) is decoupled to N reduced-order equations, each of which have 3 degree of freedom [17]. It is shown that if n (engine excitation order) is an integer, the system will only be excited at mode $n + 1$ [17]. Therefore, the steady-state response of a system with $3N$ degree of freedom is converted to the solution of a single system with 3 degree of freedom under harmonic excitation, in which case, with the exception of the constant phase, which is transferred from each sector to another sector, the blades behavior is fully identical. The constant angle ϕ_i is showed this difference.

3. NUMERICAL RESULTS AND DISCUSSIONS

Equations of motion are derived and decoupled and the system frequency response is examined. The design variables and the values used for the derivation of the system frequency response for representative model with $N = 10$ sectors and order $n = 3$ excitation, are limited according to the Table 2. In order to examine the effect of absorber, amplitude of frequency response curve of blade (system with 2 degree of freedom and without the absorber) is depicted in the Fig. 3.

The area under frequency response curve of system without absorber is represented in the Table 3 (row 2). The main goal of this investigation is to reduce this area as a criterion of dissipated energy during vibration [19]. Reduction of this area or in the other word, the minimization of vibration of the system, will prevent the phenomenon of High Cycle Fatigue. In the Table 3, S represents the area under the system frequency response's curve, and the reduction percent of dissipated energy in relative to the system without the absorber is defined as below

$$\mathcal{R} = \frac{S_{\text{without absorber}} - S_{\text{current}}}{S_{\text{without absorber}}} \times 100 \quad (16)$$

Next, the mass of absorber is considered. The system frequency response is illustrated in Fig. 4.

This condition, is shown circumstances in which, the damping of absorber is increased to the point that it is prevented the movement of absorber in relative to the blade, and in fact, the absorber is locked in its zero positions relative to the blade. The mass, length of the link of the absorber and the area under the frequency response curve of system are summarized in the Table 3 (row 3). From the Fig. 4, it is observed that the addition of the absorber mass, is shifted resonance frequencies and change maximum amplitude in the resonance condition. These conditions with principles of frequency analysis of general systems that, when total mass is increased and its stiffness remain constant and therefore system natural frequencies are reduced, have matched.

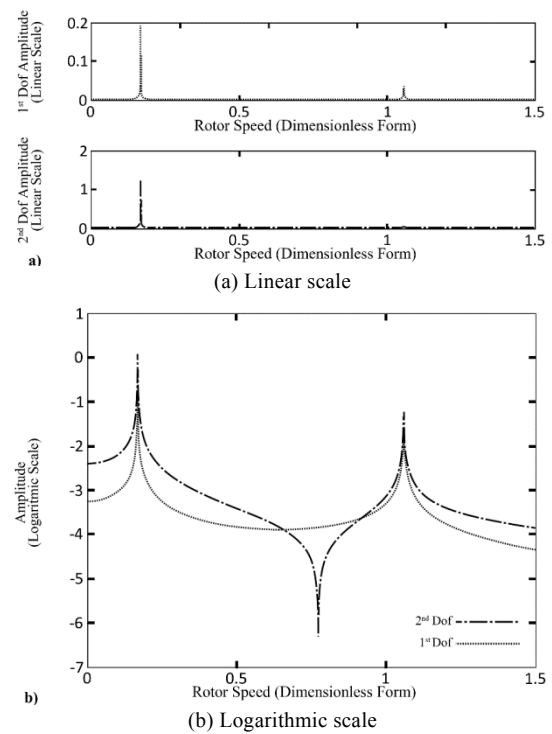


Fig. 3 Amplitude frequency response versus rotor speed (in dimensionless form) for system without absorber.

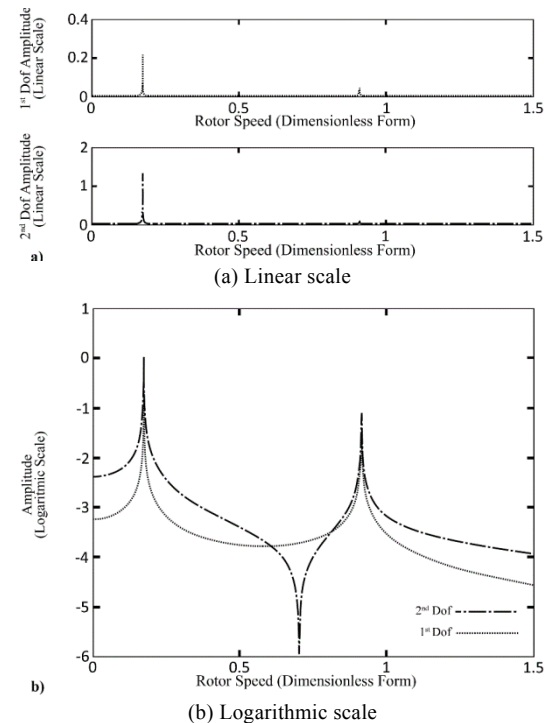


Fig. 4 Amplitude frequency response versus rotor speed (in dimensionless form) when absorber is locked in its zero positions relative to the blade.

Table 3 Dimensionless data to accompany Fig. 4 ~ 7, related area under the system frequency response curve and reduction of dissipated energy in relative to the system without the absorber.

| Row | Fig No. | Parameters | | | | S (Area under the system frequency response curve) | \mathcal{R} (Reduction of dissipated energy in relative to the system without the absorber) |
|-----|---------|---|--|--|--------|---|--|
| | | $\mu_{\bar{b}}$ (mass of the absorber) | $\rho_{\bar{b}}$ (length of the pendulum of the absorber) | $\zeta_{\bar{b}}$ (damping of the absorber) | | | |
| 1 | Fig 3. | 0 | 0 | 0 | 0.132 | 0% | |
| 2 | Fig 4. | 0.001 | 0.1 | $\zeta_{\bar{b}} \rightarrow \infty$ | 0.0406 | 69% | |
| 3 | Fig 5. | 0.001 | 0.11 | 0.01 | 0.0676 | 48% | |
| 4 | Fig 6. | 0.001 | 0.15 | 0.001 | 0.0534 | 59% | |
| 5 | Fig 7. | 0.005 | 0.15 | 0.001 | 0.0491 | 63% | |
| 6 | Fig 8. | 0.00862 | 0.128 | 7.3e-3 | 0.0206 | 84% | |

The dissipated energy is reduced by almost 70% in relative to the previous condition. In order to examine the effects of absorber parameters on the system vibration, amplitude of frequency response curve of system are illustrated in the Figs. 5 and 6 as a function of rotor speed in dimensionless form and for different values of absorber parameters. Table 3 (row 3) shows the related values of parameters of absorber, the area under the frequency response curve and the dissipated energy in relative to the system without the absorber for Fig. 5.

From Fig. 5 it is observed that the damped absorber with the values in Table 3 (row 3) is increased the system maximum amplitude under resonance condition. This is when the area under the frequency response curve is reduced than the system without absorber, and is increased than the condition in which, the absorber, is locked relative to the blade.

From the Fig. 6 it is observed that the damped order-tuned vibration absorber reduces the system maximum amplitude in the resonance condition. From the Table 3 (row 4), the area under the frequency response curve is reduced than the system without the absorber and with the absorber with different values (which is mentioned in row 3 of Table 3) while it is increased than the situation in which, the absorber is locked relative to the blade.

In row 5 of Table 3, values for the absorber's damping and length of the pendulum are constant (in relative to row 4) but the mass of the absorber is increased. Figure 7 presents the amplitude of the frequency response of the system for mentioned situation.

It is shown that with the change of absorber parameters values, the maximum amplitude and the area under the frequency response curve of the system are changed; such that, the change one of the values are reduced the

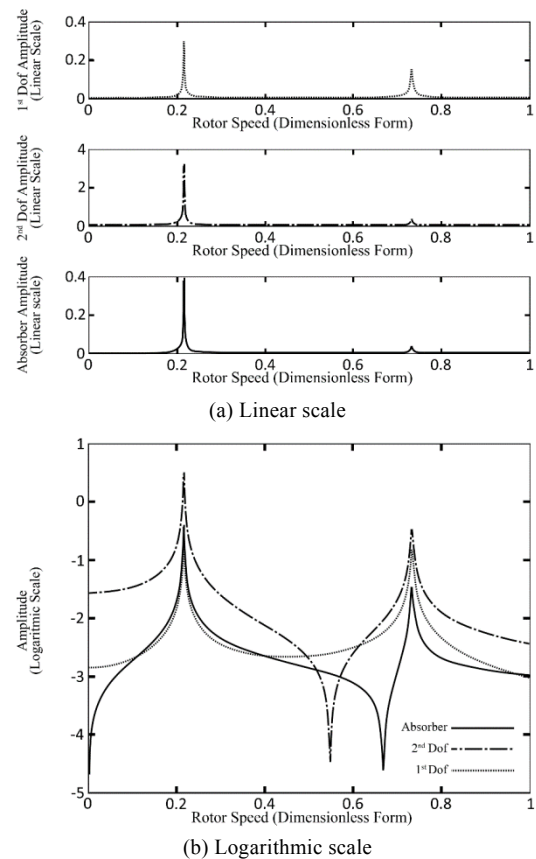


Fig. 5 Amplitude frequency response versus rotor speed (in dimensionless form) for values mentioned in row 3 of Table 3.

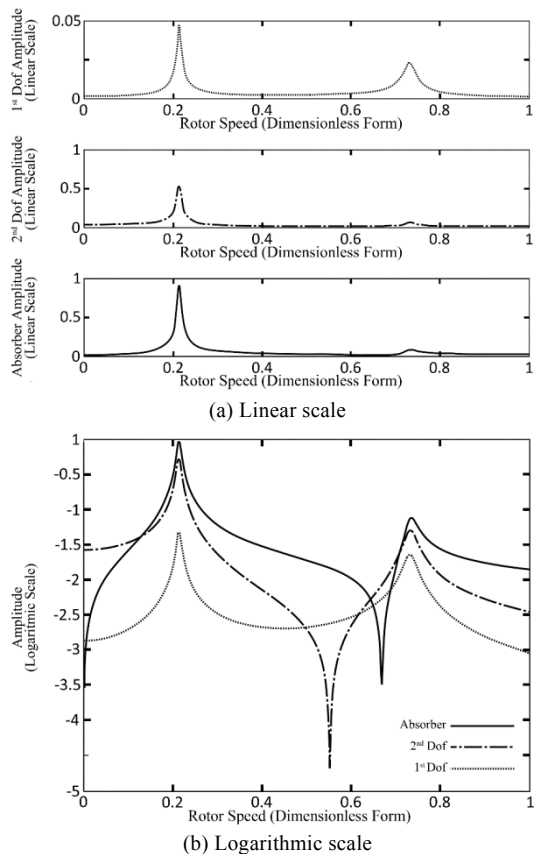


Fig. 6 Amplitude frequency response versus rotor speed (in dimensionless form) for values mentioned in row 4 of Table 3.

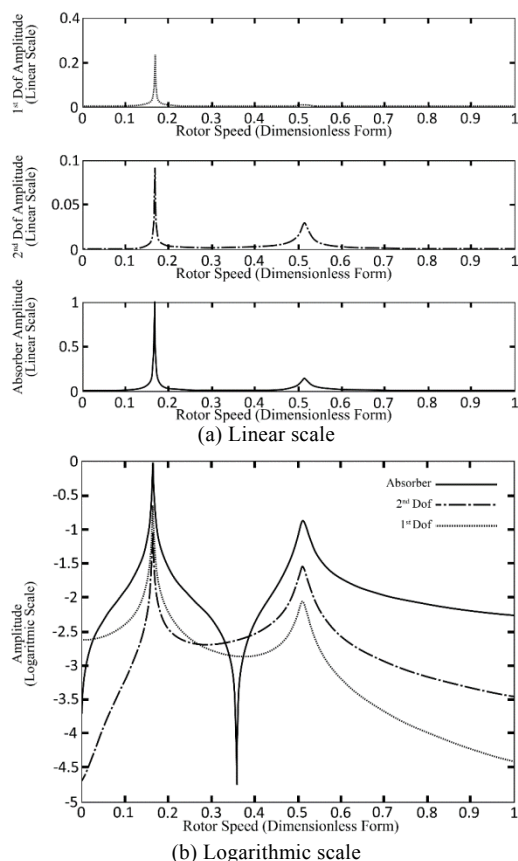


Fig. 7 Amplitude frequency response versus rotor speed (in dimensionless form) for values mentioned in row 5 of Table 3.

system amplitude and increased the area under the frequency response curve. This is when with another change the resonance is increased and the area is reduced. In order to remove system resonant peaks and minimize the energy loss resulting from blade vibration, the optimal values of absorber parameters are determined. At this part of investigation, GA runs for 2000 generations. In each generation two individuals, which are the best in terms of their fitness value, are selected as Elite children and survive to the next generation. Heuristic crossover is used. Adaptive feasible is chosen as mutation function and the initial population contains 120 individual that is compatible with design variable bounds. With the use of the H₂ optimization criterion [19], the optimal values of the absorber parameters are extracted. The aim of this criterion is to reduce the total vibration energy of the system over all frequency. In this method, the area under the curve of the frequency response of the system is minimized.

Figure 8 shows the optimal amplitude frequency response of the system, and the Table 3 (row 6) shows the optimal values of absorber parameters and the area under the frequency response curve. It is clear that the amplitude is significantly reduced under resonance conditions. The area under the frequency response curve is reached its minimum value. The dissipated energy is reduced by almost 84% in relative to system without absorber. For above conditions the absorber, is designed based on the specifications of the Table 3 (row 6), is an optimal one.

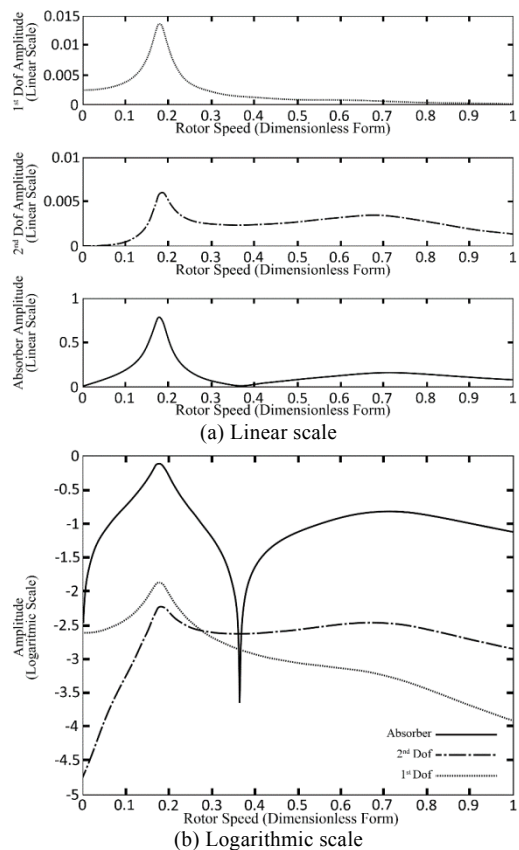


Fig. 8 Amplitude frequency response versus rotor speed (in dimensionless form) for optimal parameters, which mentioned in row 6 of Table 3.

In order to investigate the effect of values of each optimal parameters, they are changed. Table 4 shows the effects of the change of absorber damping under conditions in which, the length of the absorber pendulum and its mass are constant. In the following, \mathcal{D} represents the increase percent of the dissipated energy during blade vibration in relative to the optimal condition and is defined as below

$$\mathcal{D} = \frac{S_{\text{current}} - S_{\text{optimal}}}{S_{\text{optimal}}} \times 100 \quad (17)$$

It is shown that the area under the curve of the system frequency response is changed. It is in one step, reduced the area, and increased it under other conditions. It is observed that the smallest area is related to the optimal values of the absorber parameters. This is in a case in which with the increase of the damping of the absorber, that is, by moving towards a direction in which, the absorber is locked in relative to the blade, the area under the system frequency response curve is remained constant.

According to the Table 4, it is clear that the area under the system frequency response is extremely dependent on the damping of the absorber and with the change of absorber's damping the system response is deviated from the optimal condition. Therefore ignorance of the effect of damping of the absorber in frequency response of system (which were done in [17,18]) or considering negligible values for absorber's damping is increased the dissipated energy and maximum value of amplitude of frequency response of system.

Table 5 shows the effects of the change of pendulum's length of absorber under a condition in which, its mass and damping is constant.

According to the Table 5, it is observed again that the area under the system frequency response is dependent on the length of pendulum of absorber and with the change of the its value; the dissipated energy is deviated from the optimal condition. It is clear that the smallest area is related to the optimal values of the absorber parameters. Table 6 shows the effects of the change of the absorber mass under conditions in which the pendulum's length and damping of the absorber are constant. It is observed that the change of the mass of the absorber is deviated the system response from its optimal condition. With the change of each of the absorber's parameters, the system response is deviated from the optimal conditions. It is clear that if one of the absorber parameters is selected, there will be the possibility of optimizing two other parameters. Since in literature [17,18], the mass of the absorber is considered as a relative to the main mass, but in this investigation, the values' of the absorber mass and two other parameters are changed and determined optimally. To confirm the validity of the used method and to emphasize on the results of this investigation, the results of Gozen and colleagues [18] are examined. Definitions and values in [18] are assembled on the formulas and methods of this investigation and results are obtained and compared with results of [18] in Fig. 9.

Table 4 Different dimensionless values for absorber damping while other parameters are constant.

| $\mu_{\bar{b}}$ (Mass of the absorber) | $\rho_{\bar{b}}$ (Length of the pendulum of the absorber) | $\xi_{\bar{b}}$ (Damping of the absorber) | S (Area under the system frequency response curve) | \mathcal{D} (Increase percent of the dissipated energy in relative to the optimal condition) |
|---|--|--|---|---|
| 0.00862 | 0.128 | 7.3e-6 | 0.0598 | 65% |
| 0.00862 | 0.128 | 7.3e-5 | 0.0480 | 130% |
| 0.00862 | 0.128 | 7.3e-4 | 0.0431 | 109% |
| 0.00862 | 0.128 | 7.3e-3 | 0.0206 | 0% |
| 0.00862 | 0.128 | 7.3e-2 | 0.0681 | 230% |
| 0.00862 | 0.128 | 7.3e-1 | 0.0532 | 158% |
| 0.00862 | 0.128 | 7.3e1 | 0.073 | 270% |
| 0.00862 | 0.128 | 7.3e2 | 0.0763 | 270% |

It is necessary to mentioned that they have assigned 1 DOF to the disk and another one to the blade and by considering the undamped absorber and disregarding the effects of aerodynamic damping and by defining the parameter of β as the absorber detuning parameter, have extracted the system frequency response for different condition. Results are matched and accuracy of this investigation is approved.

Table 5 Different dimensionless values for absorber pendulum length while other parameters are constant.

| $\mu_{\bar{b}}$ (Mass of the absorber) | $\rho_{\bar{b}}$ (Length of the pendulum of the absorber) | $\xi_{\bar{b}}$ (Damping of the absorber) | S (Area under the system frequency response curve) | \mathcal{D} (Increase percent of the dissipated energy in relative to the optimal condition) |
|---|--|--|---|---|
| 0.00862 | 0.01 | 7.3e-3 | 0.0705 | 242% |
| 0.00862 | 0.04 | 7.3e-3 | 0.0694 | 236% |
| 0.00862 | 0.06 | 7.3e-3 | 0.0632 | 206% |
| 0.00862 | 0.1 | 7.3e-3 | 0.0574 | 170% |
| 0.00862 | 0.128 | 7.3e-3 | 0.0206 | 0% |
| 0.00862 | 0.13 | 7.3e-3 | 0.0309 | 33% |
| 0.00862 | 0.14 | 7.3e-3 | 0.0621 | 201% |
| 0.00862 | 0.15 | 7.3e-3 | 0.0457 | 121% |

Table 6 Different dimensionless values for absorber mass while other parameters are constant.

| $\mu_{\bar{b}}$ (Mass of the absorber) | $\rho_{\bar{b}}$ (Length of the pendulum of the absorber) | $\xi_{\bar{b}}$ (Damping of the absorber) | S (Area under the system frequency response curve) | \mathcal{D} (Increase percent of the dissipated energy in relative to the optimal condition) |
|---|--|--|---|---|
| 0.001 | 0.128 | 7.3e-3 | 0.0311 | 50% |
| 0.003 | 0.128 | 7.3e-3 | 0.0485 | 135% |
| 0.005 | 0.128 | 7.3e-3 | 0.0612 | 197% |
| 0.007 | 0.128 | 7.3e-3 | 0.0324 | 57% |
| 0.00862 | 0.128 | 7.3e-3 | 0.0206 | 0% |
| 0.009 | 0.128 | 7.3e-3 | 0.0278 | 34% |
| 0.0095 | 0.128 | 7.3e-3 | 0.0502 | 143% |
| 0.01 | 0.128 | 7.3e-3 | 0.0854 | 314% |

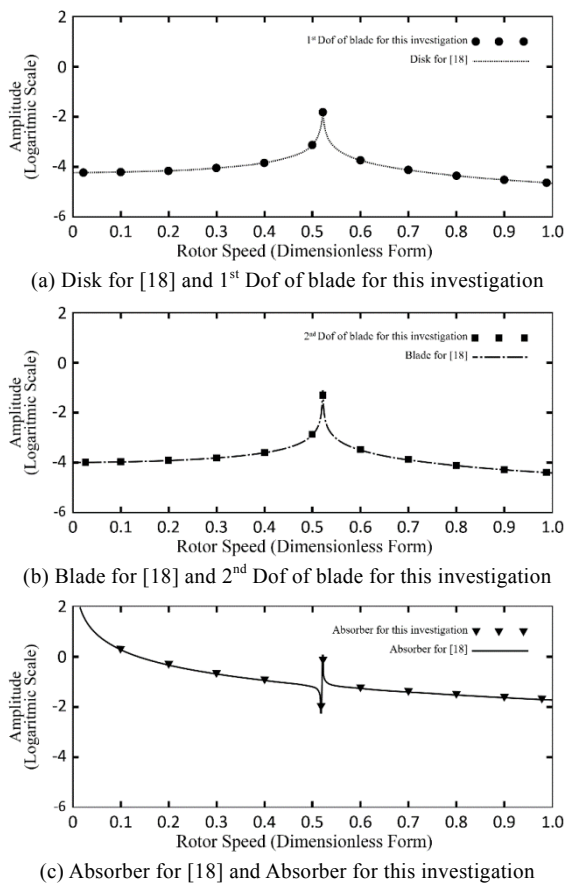


Fig. 9 Comparison of amplitude frequency response (Logarithmic scale) versus rotor speed (in dimensionless form) from Gozen and *et al.* [18] and this investigation.

4. CONCLUSIONS

In this research, the damped order-tuned vibration absorber effects on the vibration of flexible rotating blades such as turbine blades *etc.* were investigated. The system was considered as a rotationally periodic of N identical, identically-coupled blades, which were uniformly connected to a rigid disk. Lumped parameter method was used and a model with two degree of freedom of the blade were extracted and each blade was implanted with a damped centrifugally driven order-tuned vibration absorber which was moved in a circular path. The damping of the absorber was modelled by a torsional damper, which was acted at attachment point of absorber pendulum to the blade. The system frequency response was compared without the absorber and with condition in which the absorber was locked in its zero position in relative to the blade. The recent situation was shown the status in which the absorber cannot move in relative to the blade due to its excessive damping. The system frequency response curve was studied for different values of absorber parameters and the optimal values of the absorber parameters were determined by using GA and MATLAB software. In order to determine optimal values, the H_2 optimization criterion was used. In this criterion, the area under the frequency response curve as a criterion of dissipated

energy is minimized during vibration. If the values of one of the absorber parameters were changed, the system response was deviated from its optimal condition. It is concluded that all of the absorbers' design parameters including its mass, length of the pendulum and its damping have certain effects on the system frequency response and on the dissipated energy during vibration. Therefore ignorance of one of those parameters (which was happened in [17,18] and for absorber damping) is affected the system response completely. The accuracy of the results of this research was confirmed by investigating the results of relevant literature. As was mentioned the designed absorber is only capable of removing one of the system resonances. For this purpose, it seems necessary to do future works in which each blade is equipped with two or more absorbers. In this research, the absorber was moved in a circular path, so the investigation of the effects of the movement of the absorber under conditions in which it is moving in a desired way, is recommended. Although in relevant literature, some studies have been performed in which, the effects of impact absorber are investigated [20], but it seems necessary to conduct experimental studies to more accurately measure the validity of the results and to more accurately design absorber. Finally, the investigation of the effects of mistuning as an important factor in determining the behavior of the system and absorber is very important.

REFERENCES

1. Bhagi, L. K., Gupta, P. and Rastogi, V., "Fractographic Investigations of the Failure of L-1 Low- Pressure Steam Turbine Blade," *Case Studies in Engineering Failure Analysis*, **1**, pp. 72–78 (2013).
2. Yang, B., "Blade Containment Evaluation of Civil Aircraft Engines," *Chinese Journal of Aeronautics*, **26**, pp. 9–16 (2013).
3. Chou, J. S., Chiu, C. K., Huang I. K. and Chi, K. N., "Failure Analysis of Wind Turbine Blade Under Critical Wind Loads," *Engineering Failure Analysis*, **27**, pp. 99–118 (2013).
4. Faudot, C. and Dahlhaug, O. G., "Prediction of Wave Loads on Tidal Turbine Blades," *Energy Procedia*, **20**, pp. 116–133 (2012).
5. Poursaeidi, E., Babaei, A., Mohammadi Arhani, M. R. and Arablu, M., "Effects of Natural Frequencies on the Failure of R1 Compressor Blades," *Engineering Failure Analysis*, **25**, pp. 304–315 (2012).
6. Rao, R. and Dutta, B. K., "Vibration Analysis for Detecting Failure of Compressor Blade," *Engineering Failure Analysis*, **25**, pp. 211–218. (2012).
7. Astle, C., *et al.*, "Timber for Small Wind Turbine Blades," *Energy for Sustainable Development*, **17**, pp. 671–676 (2013).
8. Taplak, H. and Parlak, M., "Evaluation of Gas Turbine Rotor Dynamic Analysis Using the Finite Element Method," *Measurement*, **45**, pp. 1089–1097. (2012).

9. Luo, R., "Free Transverse Vibration of Rotating Blades in a Bladed Disk Assembly," *Acta Mechanica*, **223**, pp. 1385–1396 (2012).
10. Ewins, D. J., "Vibration Characteristics of Bladed Disc Assemblies," *Journal of Mechanical Engineering Science*, **15**, pp. 165–186 (1973).
11. Chellil, A., Noura, A., Lecheba, S., Kebirb, H. and Chevalier, Y., "Impact of the Fuselage Damping Characteristics and the Blade Rigidity on the Stability of Helicopter," *Aerospace Science and Technology*, **29**, pp. 235–252 (2013).
12. Kaneko, Y., Ohta, M., Mori, K. and Ohyama, H., "Study on Vibration Response Reduction of Bladed Disk by Use of Asymmetric Vane Spacing," *International Journal of Gas Turbine, Propulsion and Power Systems*, **4**, pp. 35–42 (2012).
13. Rastogi, V., Kumar, V. and Bhagi, L. K., "Dynamic Modeling of Underplatform Damper Used in Turbomachinery," *International Scholarly and Scientific Research & Innovation*, **6**, pp. 460–469 (2012).
14. Pennacchi, P., Chatterton, S., Bachschmid, N., Pesatori, E. and Turozzi, G., "A Model to Study the Reduction of Turbine Blade Vibration Using the Snubbing Mechanism," *Mechanical Systems and Signal Processing*, **25**, pp. 1260–1275 (2010).
15. Hollkamp, J. J., Bagley, R. L. and Gordon, R. W., "A Centrifugal Pendulum Absorbers for Rotating Hollow Engine Blades," *Journal of Sound and Vibration*, **219**, pp. 539–549 (1999).
16. Shaw, S. W. and Pierre, C., "The Dynamic Response of Tuned Impact Absorbers for Rotating Flexible Structures," *Journal of Computational and Nonlinear Dynamics*, **1**, pp. 13–25 (2006).
17. Olson, B. J., "Order-Tuned Vibration Absorbers for Systems with Cyclic Symmetry with Applications to Turbomachinery," Ph.D. Dissertation, Department of Mechanical Engineering, Michigan State University, Michigan, U.S.A. (2006).
18. Gozen, S., Olson, B. J., Shaw, S. W. and Pierre, C., "Resonance Suppression in Multi-Dof Rotating Flexible Structures Using Order-Tuned Absorbers," *Journal of Vibration and Acoustics*, **134**, pp. 845–854 (2012).
19. Asami, T., Nishihara, O. and Baz, A. M., "Analytical Solutions to H_∞ and H_2 Optimization of Dynamic Vibration Absorbers Attached to Damped Linear Systems," *Journal of Vibration and Acoustics*, **124**, pp. 284–295 (2002).
20. Duffy, K. P., Bagley, R. L. and Mehmed, O., "On a Self-Tuning Impact Vibration Damper for Rotating Turbomachinery," Technical Report, National Aeronautics and Space Administration (2000).

(Manuscript received April 13, 2015,
accepted for publication December 6, 2015.)